

# RIP1 upregulation promoted tumor progression by activating AKT/Bcl-2/BAX signaling and predicted poor postsurgical prognosis in HCC

Cong Wang<sup>1</sup> · Bowen Yao<sup>1</sup> · Meng Xu<sup>1</sup> · Xin Zheng<sup>1</sup>

Received: 13 June 2016 / Accepted: 6 September 2016 / Published online: 4 October 2016  
© International Society of Oncology and BioMarkers (ISOBM) 2016

**Abstract** Although growing body of evidences have identified a critical role for receptor-interacting protein kinase 1 (RIP1) in mediating cell death signaling, its possible contribution to hepatocellular carcinoma (HCC) progression remains unclear. Here, we displayed that expression of RIP1 was significantly upregulated in HCC tissues than in adjacent liver tissues from 81.9 % HCC patients ( $P < 0.001$ ) by immunohistochemistry (IHC) staining. Overexpression of RIP1 was found positively associated with HBV infection, advanced TNM staging, portal vein invasion, and intrahepatic metastases. Kaplan-Meier curve analysis indicated that patients with higher RIP1 expression in HCC tissues suffered from unfavorable postsurgical survival. Higher RIP1 expression in HCC tissues was also confirmed to be an independent poor prognostic predictor. Knockdown of RIP1 resulted in suppression of cell viability and proliferation and induced cell apoptosis in MHCC97h cells. Nevertheless, enforced expression of RIP1 promoted cell viability and proliferation of Huh7 cells and inhibited cell apoptosis. Mechanistic studies revealed that RIP1 exerted its function on HCC progression via activating

AKT/Bcl-2/BAX signaling. In conclusion, our results provided the evidence of RIP1 overexpression in HCC, and RIP1 could be a novel predictive factor of unfavorable prognosis in HCC patients. Activation of AKT/Bcl-2/BAX signaling contributed to RIP1 promoting HCC progression.

**Keywords** RIP1 · HCC · AKT · Bcl-2/BAX · Prognosis

## Introduction

Hepatocellular carcinoma (HCC) is the most common type of primary liver cancer, with a reported estimated 782,500 new liver cancer cases and 745,500 related deaths worldwide in 2012 [1]. Although there have been a variety of remarkable improvements in treatment of this neoplasm including surgical resection, radiotherapy, and chemotherapy during the last few decades, the prognosis of patients with HCC is far from desirable due to the high risk of recurrence and distant metastasis. Limited liver donor restricted the application of liver transplantation on the treatment of HCC. Nevertheless, due to the absence of symptoms and rapid tumor progression and invasion during the early stages, patients were commonly diagnosed with HCC at the advanced stage [2], which resulted to that most of HCCs were not suitable to receive radiofrequency ablation. Liver resection is still considered as the most important curative therapy for HCC patients [3]. Unfortunately, different patients suffered from various outcomes after liver resection [4, 5]. Therefore, it is not only necessary but also emerging to identify the effective postsurgical predictive factors for HCC patients, uncover the underlying mechanism of tumor recurrence and metastases after liver resection, and develop the relevant novel therapeutic regimen.

---

Cong Wang and Bowen Yao contributed equally to this work.

---

✉ Xin Zheng  
raymondzhengxin@foxmail.com

Cong Wang  
wangcongwa@126.com

Bowen Yao  
ybwsplendid@126.com

Meng Xu  
987556919@foxmail.com

<sup>1</sup> Department of Hepatobiliary Surgery, The First Affiliated Hospital of Xi'an Jiaotong University, 277 Yanta West Road, Xi'an, Shaanxi 710061, China

Receptor-interacting protein kinase 1 (RIP1) is one of the RIP family containing seven different members with a homologous kinase domain but different functional domains [6]. It has already been found that three domains with different function constitutes RIP1 protein construction including the N-terminal kinase domain involved in necroptosis, the C-terminal domain contributing to induction of apoptosis, and an intermediate domain essential for activation of NF $\kappa$ B signaling [7–9]. It was reported that RIP1-deficient mice showing extensive apoptosis in lymphoid tissue died at 1–3 days of age [10], which validated that RIP1 was indispensable to mediate cell death and maintain the homeostasis of a tissue or organism. The binding of TNF $\alpha$  to its receptor brings about two different results, an inflammatory response or cell death. With the existence of RIP1, TNF $\alpha$  results in the formation of initial and second plasma membrane-bound complex (complex I and II). Complex I is comprised of TNF-R1, TRAF2, TRADD, cIAP1, and RIP1, which increase the expression of various antiapoptotic proteins including TRAF1, TRAF2, cIAP1, cIAP2, and cellular FADD-like IL-1 $\beta$ -converting enzyme inhibitory protein via activating different cell signal pathways including NF $\kappa$ B and MAPKs/ERK signaling [11–13]. In case that complex I fails to activate NF $\kappa$ B signaling, complex II also promotes cell apoptosis through upregulation of both FADD and caspase-8 [14, 15]. Hence, RIP1 exerts a dual function on modulating cell apoptosis.

In the present study, we observed that RIP1 expression was aberrantly increased in HCC tissues and overexpression of RIP1 in HCC was positively associated with poor outcome after liver resection. And, further mechanism studies revealed that RIP1 repressed HCC cell apoptosis through AKT/Bcl2/BAX axis.

## Materials and methods

### Patients and specimens

The study was reviewed and approved by the ethics committee of the First Affiliated Hospital of Xi'an Jiaotong University according to the Helsinki Declaration of 1975 (no. 20080301, 6 May 2008). A total of 210 patients who received curative resection for HCC by the same surgical team in Department of Hepatobiliary Surgery at the First Hospital of Xian Jiaotong University from January 2004 to June 2007 were recruited in this study. All patients enrolled here have signed informed consent to participate in this investigation and for publication. None of the patients received any neoadjuvant chemotherapy or radiotherapy before liver resection. The median age of patients was 53 years old, ranging from 27 to 75 years old. TNM staging was determined according to the seventh edition of AJCC/UICC classification system. HCC tissue and matched adjacent liver tissue specimens

(>2-cm distance to the resection margin) were harvested during liver resection and immediately stored at paraformaldehyde for immunohistochemistry staining assay. Two experienced pathologists blinded to the clinical information provided the histopathologic information including Edmonson-Sternier classification, TNM grading, and tumor diameter. The follow-up information was obtained from 175 of 210 HCCs (83.3 %) with median follow-up time of 42.5 months, ranging from 3 to 75.4 months. The clinical information of HCC patients is presented in Table 1.

### Immunohistochemistry staining assay

We conducted the immunohistochemistry (IHC) staining assay as described in the previous study [16]. IHC staining assay was performed on 4- $\mu$ m thick paraformaldehyde-fixed paraffin sections. Briefly, after being deparaffinized in xylene and rehydrated, the slide was incubated in 0.3 % hydrogen peroxide for half an hour to block endogenous peroxidase activity. After antigen retrieval in sodium citrate buffer for 45 s, the slide was blocked overnight at 4 °C. Next, the slide was incubated with the primary antibody against RAP1 (Catalog No.: ab72139, Abcam, USA) at 4 °C overnight, which was then detected with the biotinylated secondary antibody (Boster, China). The staining of the slide was carried out using the avidin-biotin-peroxidase complex. Finally, the sections were visualized with diaminobenzidine and counterstained with hematoxylin.

Each slide was independently observed by two experienced pathologists. Staining intensity was scored using four grades (0–3): 0 (negative), 1 (weakly positive), 2 (moderately positive), and 3 (strongly positive). The percentage of positive cells was also scored using five categories (0–4): a score of 0 was given for 0–5 %, 1 for 6–25 %, 2 for 26–50 %, 3 for 51–75 %, and 4 for >75 %. The final staining score was obtained by multiplying the staining intensity and the percentage of positive cells.

### Cell cultures

Three HCC cell lines including Hep3B and HepG2 were purchased from the American Type Culture Collection (Manassas, VA, USA). The human immortalized normal hepatocyte cell line LO2 was purchased from the Institute of Biochemistry and Cell Biology, Chinese Academy of Sciences (Shanghai, China). Both Huh7 and MHCC97h cell lines were obtained from Prof. Kefeng Dou (Department of Hepatobiliary Surgery, Xijing Hospital, Fourth Military Medical University) as kind gifts. LO2, Huh7, MHCC97h, and Hep3B cells were cultured in DMEM medium with 10 % FBS. HepG2 cells were cultured in RPMI 1640 medium with 10 % FBS.

**Table 1** Demographic information and clinicopathological features of 175 HCC patients with the follow-up information

Clinicopathological features		No. of patients		$\chi^2$	P value
		High RIP1	Low RIP1		
Age (years)	<50	65	11	0.004	0.950
	$\geq$ 50	85	14		
Gender	Male	97	13	2.411	0.121
	Female	53	12		
HBV infection	Present	116	14	5.105	0.024
	Absent	34	11		
Serum AFP level (ng/mL)	<400	32	7	0.549	0.458
	$\geq$ 400	118	18		
Tumor size (cm)	<5	64	10	0.092	0.762
	$\geq$ 5	86	15		
Liver cirrhosis	Present	137	21	1.314	0.252
	Absent	13	4		
Edmondson-Steiner Classification	I + II	62	15	3.030	0.082
	III + IV	88	10		
TNM stage	I + II	44	16	11.430	0.001
	III + IV	106	9		
Portal vein invasion	Present	48	3	4.151	0.042
	Absent	102	22		
Intrahepatic metastases	Present	35	1	4.902	0.027
	Absent	115	24		

### Quantitative RT-PCR

The total RNA of HCC cells was isolated in accordance with the manufacturer's instructions included in the RNeasy kit from Qiagen Co. (Valencia, USA). cDNA synthesis and qRT-PCR analysis (TaqMan gene expression assay) were carried out as described previously [17]. The ABI TaqMan probes (Applied Biosystems, USA) targeting (Hs01041868\_m1) and 18 s rRNA (Hs99999901\_s1) were used here. There were six replicates in each measurement and the examination was repeated three times.

### Western immunoblotting

Western immunoblotting was carried out according to the protocol described in our previous report [18]. Briefly, 30 mg of denatured protein samples harvested from HCC cells were separated by polyacrylamide gel electrophoresis (PAGE), transferred into a PVDF membrane, and incubated overnight respectively with the primary antibodies against RAPI (catalog no.: ab72139, Abcam, USA), pan-AKT (catalog no.: ab8805, Abcam, USA), phos-AKT (catalog no.: ab38449, Abcam, USA), Bcl-2 (catalog no.: ab32124, Abcam, USA), and BAX (catalog no.: ab32503, Abcam, USA) at 4 °C. Protein blots were washed by Tris-buffered saline buffer with Tween (TBST) and then incubated with the relevant secondary antibodies conjugated with HRP. The results were visualized using the Thermo Pierce ECL Western Blotting Substrate

(catalog no.: 32209, USA). The level of all the proteins examined was normalized to  $\beta$ -actin.

### RNAi transfections

The siRNA sequences used here are listed as follows: RIP1 siRNA: 5'-GGA GCA AAC UGA AUA AUG AAG AGC A-3' and scramble siRNA: 5'-CAG AGA GGA GGA AAG GAG ACG CAG G-3', which was designed by Pan group [19]. Introduction of siRNAs was conducted as described previously [20]. Briefly, MHCC97h cells were seeded in six-well plates at the concentration of  $0.2 \times 10^6$  per well and grown overnight. One hundred nanomolar siRNAs was transfected into MHCC97h cells per each well using Lipofectamine RNAi MAX Reagent (Invitrogen, CA, USA). Further assessments were performed at 48 h after transfection.

### Establishment of RIP1-stable transfectant clones

The RIP1-expressing plasmid was obtained from Origene (catalog no.: RC216024) and transfected into Huh7 cells using FuGENE6 Transfection Reagent from Promega (Madison, WI, USA) as RIP1-expressing Huh7 cells (Huh7 RIP1 cells). On the other hand, the empty pCMV6 plasmid was transfected into the Huh7 cells to be Huh7 vector cells. After the 2-week selection with Geneticin (G418), the stable transfectant clones of both Huh7 RIP1 and Huh7 control cells were achieved.

## Cell apoptosis assessment

Two distinct measurements were carried out to get the convincing results of cell apoptosis in this investigation. At first, caspase 3/7 activity assay was conducted using the Apo-ONE® Homogeneous Caspase-3/7 Assay kit (catalog no.: G7792, Promega, USA) as introduced previously [21]. Second, flow cytometry assay was used to evaluate cell apoptosis with the Alexa Fluor® 488 annexin V/Dead Cell Apoptosis Kit (Invitrogen, USA) and FACSCalibur (Becton Dickinson, USA). All examinations were repeated six times.

## Cell proliferation and cell viability assays

HCC cells were plated into 96-well plates at 5000 cells per well for 24 h and ready for the examination of cell proliferation or viability. BrdU ELISA assay was performed to detect cell proliferation and 3-(4, 5-dimethylthiazol-2-yl)-2,5-diphenyl tetrazolium bromide (MTT) assay was used to evaluate cell viability at 24, 48, 72, and 96 h. Each examination included six replicates and repeated three times.

## Statistical analysis

Data were presented as the means  $\pm$  standard error of the mean (SEM). Differences between groups were compared with the Mann-Whitney U test or the Student's *t* test. Demographic information of patients from the low RIP1 and high RIP1 groups was compared by the  $\chi^2$  test. The log-rank test was used to analyze differences of the Kaplan-Meier curves

between the low RIP1 group and high RIP1 group. Multivariate analysis was carried out with SPSS V17.0 software (SPSS Inc., USA), and the PRISM 5 software (GraphPad, USA) was used for other statistical analyses. A *P* value less than 0.05 was considered statistically significant.

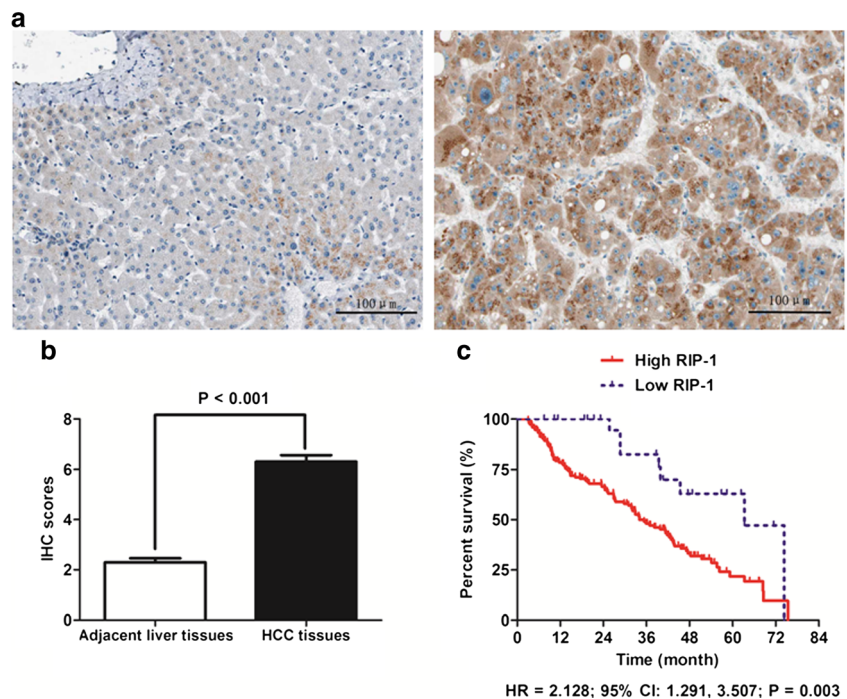
## Results

### RIP1 was overexpressed in HCC tissues and predicted the worse prognosis after liver resection

To detect expression of RIP1 in both HCC tissues and adjacent liver tissues, we examined 210 pairs of HCC specimens and adjacent liver specimens using IHC staining assay and found that RIP1 protein was located in cytoplasm predominantly, as shown in Fig. 1a. Higher RIP1 expression was observed in 81.9 % (172/210) of HCC cases. Mann-Whitney U test confirmed that this difference of RIP1 expression between HCC tissues and adjacent liver tissues was significant (Fig. 1b).

The follow-up information after surgery from 175 of the 210 HCC cases (83.3 %) was obtained. These 175 HCC patients were divided into two groups including high RIP1 group and low RIP1 group. The high RIP1 group included patients with higher RIP1 expression in HCC than in adjacent liver tissues, while the low RIP1 group contained patients with lower RIP1 expression in HCC tissues compared to adjacent liver tissues. After analyzing the clinical characteristics between high RIP1 and low RIP1 group, we found that apparently more patients from the high RIP1 group suffered from

**Fig. 1** RIP1 was overexpressed in HCC tissues and associated with poor prognosis of HCC patients after liver resection. **a** The left panel was the representative picture of RIP1 IHC staining in adjacent liver tissues, while the representative picture of RIP1 IHC staining was the right panel. **b** Mann-Whitney U test showed that there was stronger expression of RIP1 in HCC tissues than in adjacent liver tissues. **c** Comparison of Kaplan-Meier survival curves displayed that patients with higher RIP1 expression in HCC tissues suffered from the worse prognosis after liver resection



HBV infection (77.3 vs. 56.0 %,  $P = 0.024$ ), advanced TNM staging (70.7 vs. 36.0 %,  $P = 0.001$ ), portal vein invasion (28.0 vs. 12.0 %,  $P = 0.024$ ), and intrahepatic metastases (23.3 vs. 4.0 %,  $P = 0.024$ ) compared with the low RIP1 group. Subsequently, Kaplan-Meier curves were built and analyzed by log-rank test analyses to determine the association between the levels of RIP1 expression in HCC tissues and postsurgical outcome of these 175 HCCs. And, we observed that HCC patients from the high RIP1 group had the significantly shorter postsurgical overall survival than did those from the low RIP1 group (HR = 2.128; 95 % CI 1.291, 3.507;  $P = 0.003$ ; Fig. 1c). The median survival time was 62.3 months in the high RIP1 group, which was about twice those in the low RIP1 group (34.03 months). The 3-year survival rate was 48.1 % for the high RIP1 group compared with 82.6 % for the low RIP1 group. Similarly, there was a lower 5-year survival rate in the high RIP1 group (21.7 %) than that (62.9 %) in the low RIP1 group.

Univariate analysis displayed that advanced TNM staging, portal vein invasion, intrahepatic metastases, and higher RIP1 expression in tumor tissues were the worse prognosis factors (Table 2). Furthermore, portal vein invasion, intrahepatic metastases, and higher RIP1 expression in tumor tissues were established as the independent prognostic factors by multivariate Cox proportional hazard regression analysis (Table 2). These data suggested strongly that overexpression of RIP1 in HCC tissues could serve as a predictor of poor prognosis after hepatic resection.

### The expression of RIP1 in HCC cell lines

To identify the reasonable HCC cell model for the further studies, we examined the RIP1 expression in four different human HCC cell lines (Huh7, Hep3B, HepG2, and MHCC97h) and normal human immortalized hepatocyte line LO2 by both qRT-PCR and Western immunoblotting. As presented in Fig. 2a, qRT-PCR assay showed that there was less mRNA expression of RIP1 in normal human hepatocyte line LO2 than in all the other HCC cell lines. And, all four HCC cell lines expressed different RIP1 mRNAs: MHCC97h cells had the highest level of RIP1 mRNA and Huh7 cells expressed the least RIP1 mRNA. As detected by Western

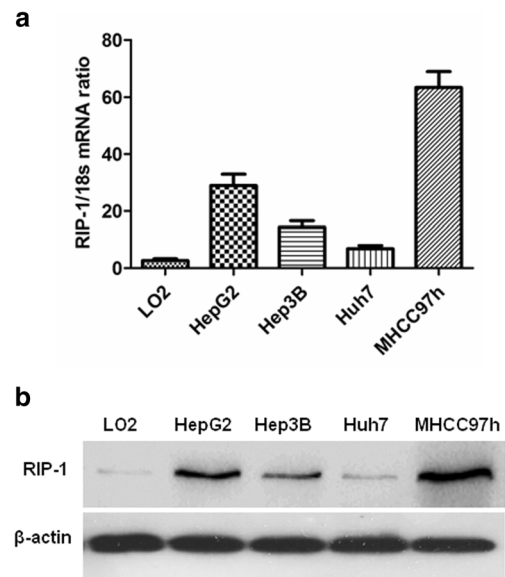


**Fig. 2** The expression of RIP1 in human normal liver cell line LO2 and four different HCC cell lines at the level of mRNA (a) and protein (b)

immunoblotting assay, the protein expression of RIP1 in all the four HCC cell lines and normal human hepatocyte LO2 mirrored the mRNA expression (Fig. 2b). Therefore, MHCC97h cells provide an excellent model for the RIP1 knockdown experiments, while Huh7 cells were selected for the RIP1 enforced-expression studies.

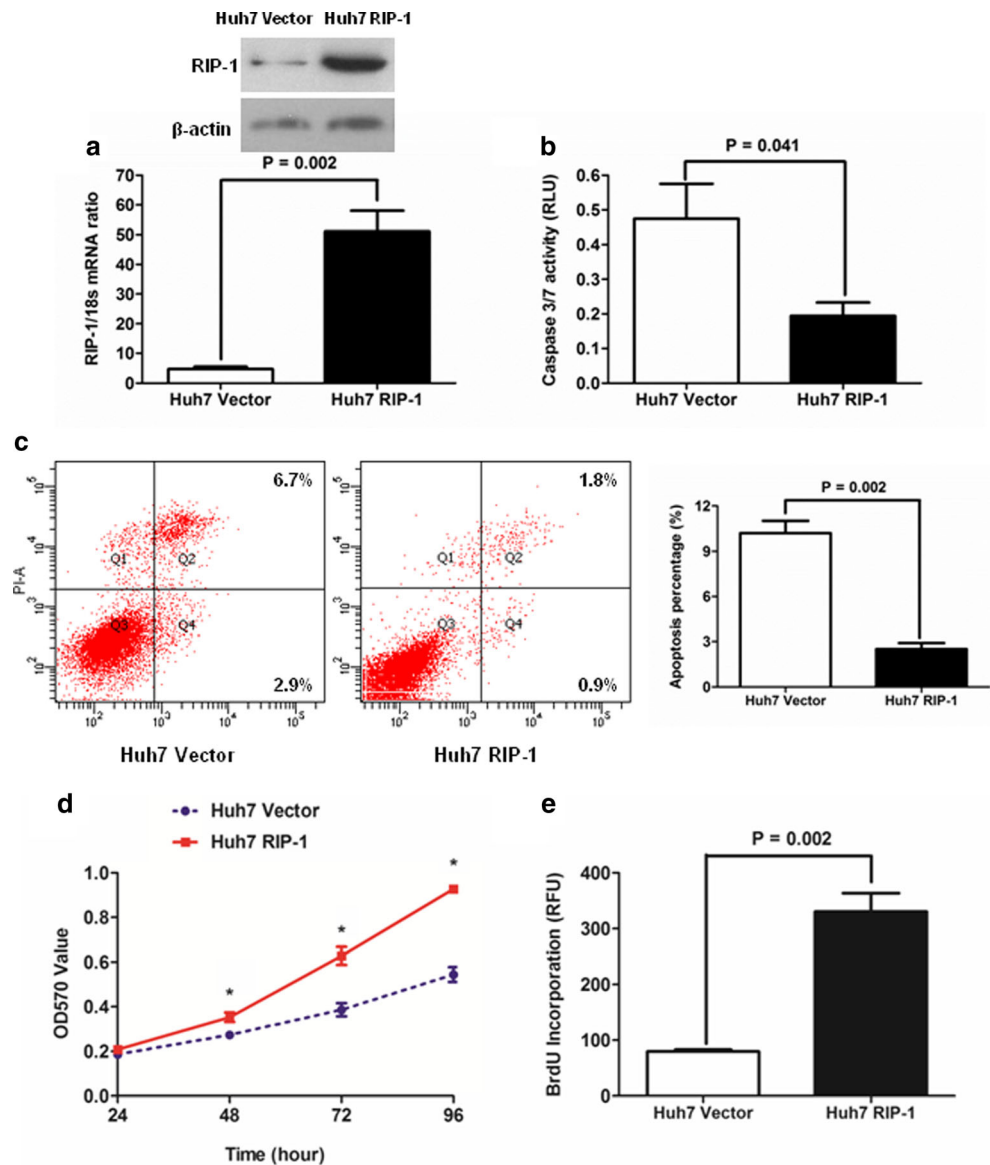
### Enhanced expression of RIP1 repressed cell apoptosis and promoted cell growth in HCC cells

To define the potential oncogenic role of RIP1 overexpression on HCC, we established Huh7 clones overexpressing RIP1 stably by transfection of RIP1 expressing plasmid. As examined by qRT-PCR and Western immunoblotting, transfection of RIP1 expressing plasmid increased the expression of RIP1 in Huh7 cells in the levels of both mRNA and protein (Fig. 3a). Caspase 3/7 activity was decreased more than two-fold in Huh7 cells by RIP1 overexpression ( $P = 0.041$ , Fig. 3b). And, flow cytometry apoptosis measurement also confirmed that the percents of apoptosis cells including both early and late apoptosis cells in Huh7 RIP1 cells were significantly less than those in the Huh7 vector cells ( $P = 0.002$ , Fig. 3c). As examined by MTT assay, RIP1 overexpression

**Table 2** Cox regression analysis of the relationship between clinicopathological features and postsurgical survival rate of HCC patients

Clinicopathological features	Univariate analysis		Multivariate analysis	
	RR (95 % CI)	<i>P</i> value	RR (95 % CI)	<i>P</i> value
Advanced TNM staging	1.632 (1.026–3.015)	0.042	1.354 (0.898–2.411)	0.081
Portal vein invasion	2.321 (1.523–3.544)	0.004	2.011 (1.341–3.017)	0.017
Intrahepatic metastases	3.215 (2.218–4.028)	0.001	3.008 (2.012–3.752)	0.005
Higher RIP1 in tumor tissue	2.496 (1.785–3.158)	0.004	2.055 (1.235–2.879)	0.008

**Fig. 3** Ectopic expression of RIP1 inhibited cell apoptosis and promoted cell viability and proliferation of Huh7 cells. **a** Both qRT-PCR and Western immunoblotting assays showed that transfection of RIP1 expressing plasmid increased RIP1 expression in Huh7 cells. **b** There was less caspase 3/7 activity in the Huh7 RIP1 cells compared with the Huh7 vector. **c** By flow cytometry apoptosis assay, it was found and confirmed that the percents of apoptosis cells including both early and late apoptosis cells in the Huh7 RIP1 cells were significantly less than those in the Huh7 vector cells. **d** MTT assay demonstrated that RIP1 overexpression promoted the viability of Huh7 cells at 48, 72, and 96 h dramatically. **e** BrdU incorporation of Huh7 cells was increased by RIP1 overexpression



apparently accelerated the viability of Huh7 cells at 48, 72, and 96 h (Fig. 3d). Consistently, BrdU incorporation of Huh7 RIP1 cells was significantly higher than of the Huh7 vector cells (Fig. 3e). These data demonstrated that RIP1 enhanced HCC cell growth and inhibited cell apoptosis.

#### Knockdown of RIP1 reinforced cell apoptosis and led to growth arrest in HCC cells

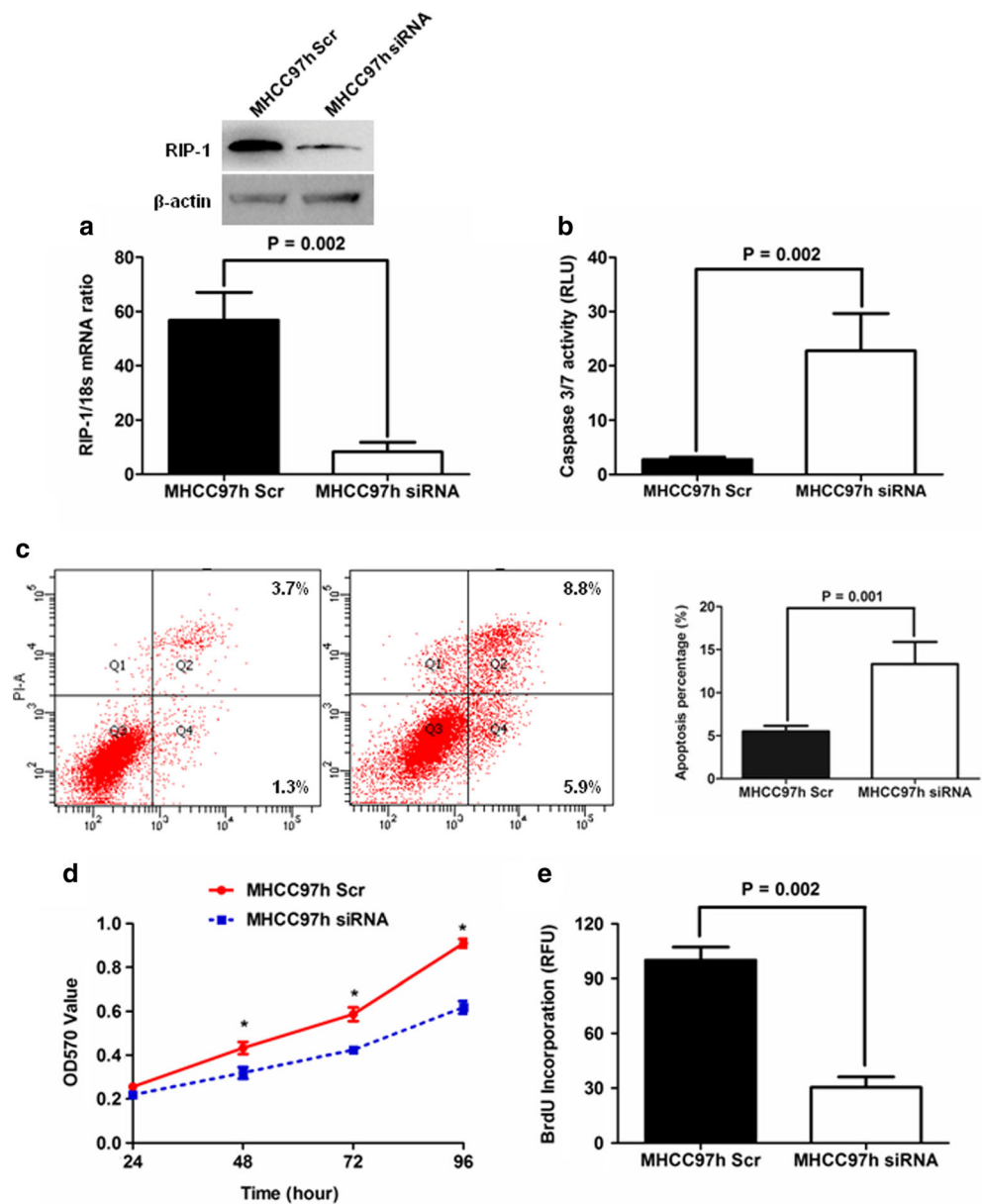
To further verify the regulatory function of RIP1 on cell apoptosis and growth of HCC cells, we silenced the RIP1 expression in MHCC97h cells with the high level of RIP1 expression with the siRNA sequences. MHCC97h cells transfected with RIP1 siRNA sequence was labeled as MHCC97 siRNA cells, while MHCC97h Scr cells were those transfected with scramble siRNA sequence. By the examination of both qRT-PCR and Western immunoblotting assays, transfection of siRNA

sequences targeting RIP1 decreased mRNA and protein expression of RIP1 in MHCC97h cells magnificantly (Fig. 4a). There was significantly more caspase 3/7 activity in MHCC97h siRNA cells than in MHCC97h Scr cells (Fig. 4b). Similarly, suppression of RIP1 also increased the apoptosis percentage of MHCC97h cells as measured by flow cytometry assay (Fig. 4c). Cell viability of MHCC97h cells was found to be repressed by knockdown of RIP1 by MTT assay (Fig. 4d). Consistent with the MTT assay, significantly more BrdU incorporation was observed in MHCC97h siRNA cells compared with MHCC97h Scr cells (Fig. 4e).

#### RIP1 promoted phosphorylation of AKT and increased the ratio of Bcl-2/BAX in HCC cells

To reveal the mechanism of the inhibitory function of RIP1 on cell apoptosis, we performed Western immunoblotting to

**Fig. 4** Knockdown of RIP1 drove cell apoptosis and attenuated cell viability and proliferation of MHCC97h cells. **a** Both qRT-PCR and Western immunoblotting assays displayed that transfection of RIP1 siRNA sequence greatly abated RIP1 expression in MHCC97h cells. **b** Caspase 3/7 activity in MHCC97h siRNA cells was more than that in MHCC97h Scr cells. **c** RIP1 upregulated the apoptosis percentage of MHCC97h cells as measured by flow cytometry assay. **d** Cell viability of MHCC97h cells was repressed by knockdown of RIP1, as assessed by MTT assay. **e** There was significantly more BrdU incorporation observed in MHCC97h siRNA cells than in MHCC97h Scr cells



examine the expression and phosphorylation of AKT in both Huh7 and MHCC97h cells. As shown in Fig. 5a, there was a significantly higher level of phosphorylation of AKT in Huh7 RIP1 cells than in Huh7 vector cells. Consistently, knockdown of RIP1 in MHCC97h cells led to apparent repression of the phosphorylation of AKT (Fig. 5b). Furthermore, we detected the regulatory effect of RIP1 on the expression of Bcl-2 and BAX which have been established as the downstream components of AKT and well-known mediators contributing to cell apoptosis. Ectopic expression of RIP1 resulted in increased expression of Bcl-2 and decreased expression of BAX in Huh7 cells (Fig. 5a). And, there was less Bcl-2 expression and more BAX expression in MHCC97h siRNA cells in contrast to MHCC97h Scr cells (Fig. 5b). Therefore, these results implied that RIP1 upregulated the Bcl-2/BAX ratio via

increasing phosphorylation of AKT and consequently inhibited cell apoptosis in HCC cells.

## Discussion

During the last few decades, RIP1 was considered to contribute to tumor suppression because it could induce apoptosis and programmed necrosis by various cellular stresses [22–24]. RIP1 was found involved in CD40 ligand-driven necroptosis-like cell death in ovarian cancer cells [25]. Xu and his colleagues discovered that RIP1 was involved in APAP-induced necroptosis in acute liver failure using the mouse model [26]; Shikonin was proven to kill glioma cells through RIP1-induced necroptosis [27]. Herein, it seems that

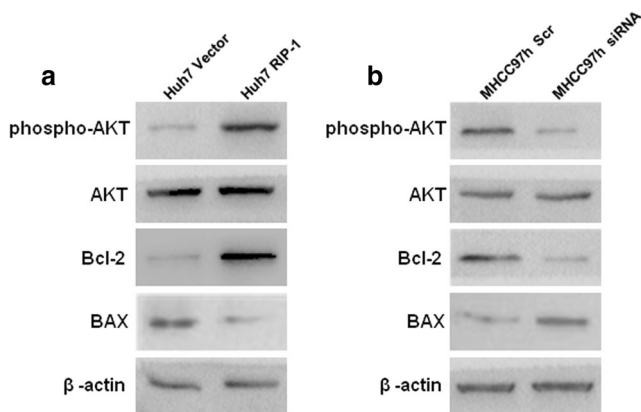


**Fig. 5** RIP1 increased the ratio of Bcl-2/BAX via phosphorylation of AKT in HCC cells. **a** Enhanced expression of RIP1 was found to result in higher level of AKT phosphorylation and increased the Bcl-2/BAX ratio in Huh7 cells by Western immunoblotting. **b** Silencing RIP1 repressed the phosphorylation of AKT and decreased the Bcl-2/BAX ratio in MHCC97h cells by Western immunoblotting

RIP1 might serve as a negative mediator of cancer pathogenesis via driving apoptosis or necrosis.

However, recently, there has been different biological function of RIP1 found in the pathogenesis of cancer. Wang's group examined the expression of RIP1 on gastric cancer and normal gastric tissues [28]. It was observed that RIP1 was overexpressed in gastric cancer tissues compared with normal gastric tissues and predicted the unfavorable prognosis of gastric cancer patients. Interestingly, positive RIP1 staining was found at the site of invasion rather than at the gastric cancer parts of interstitial substance. Further studies revealed that RIP1 knockdown inhibited cell proliferation and invasion ability of gastric cancer cells *in vitro* and suppressed the growth of gastric cancer xenografts *in vivo* via regulation of the NF- $\kappa$ B/AP-1-VEGF-C signaling. The similar results were reported in gallbladder cancer, which showed that RIP1 was aberrantly upregulated in gallbladder cancer and promoted the growth and invasion of gallbladder cancer cells by activating the NF- $\kappa$ B/AP-1-VEGF-C pathway [29]. RIP1 was also found to be commonly upregulated in melanoma, and mechanistic studies demonstrated that RIP1 attenuated cell apoptosis and then accelerated the growth of melanoma cells *in vitro* and *in vivo* via regulation of NF- $\kappa$ B signaling [30]. RIP1 was also found to inhibit cell apoptosis of leukemia cells via increasing phosphorylation of ERK1/2 [19].

In the present investigation, we observed that RIP1 was frequently upregulated in HCC tissues and associated with HBV infection, advanced TNM staging, portal vein invasion, and intrahepatic metastases. After analyzing the follow-up information with the Kaplan-Meier survival curves, we found that overexpression of RIP1 in HCC tissues was significantly correlated with the poor prognosis of HCC patients. And, the multivariate Cox proportional hazard regression test identified RIP1 as the independent prognostic factor. Enforced

expression of RIP1 attenuated cell apoptosis and promoted the growth of HCC cells. Consistently, knockdown of RIP1 enhanced cell apoptosis and inhibited cell viability and proliferation of HCC cells. Mechanistic investigation revealed that RIP1 unregulated phosphorylation of AKT, and in turn, increased the Bcl-2/BAX ratio which finally induced HCC cell apoptosis. It supported strongly that activation of AKT/Bcl-2/BAX signaling was involved closely in the inhibitory function of RIP1 on HCC cell apoptosis. However, the concrete mechanisms that RIP1 promoted HCC cell growth were not completely revealed. Our group will conduct further investigation including gene microarray and cell pathway analysis to address them.

In summary, this study demonstrated that RIP1 was aberrantly upregulated in HCC and predicted the poor prognosis of HCC patients. Moreover, we revealed here that RIP1 functioned as a novel oncogenic regulator in HCC pathogenesis rather than an antitumor mediator via AKT/Bcl-2/BAX signaling. RIP1 is potentially developed as a novel biomarker of poor prognosis in HCC patients.

**Acknowledgments** This study was supported by grants from the National Natural Scientific Foundation of China (81301743 and 81572733 to Xin Zheng), Research Fund for the doctoral Program of High Education of China from Ministry of Education (no. 201202011120090 to Xin Zheng), Key Science and Technology Program of Shaanxi Province (no. 2014K11-01-01-21 to Xin Zheng), and the Fundamental Research Funds for the Basic Research Operating expenses Program of Central College sponsored by Xi'an Jiaotong University to Xin Zheng.

#### Compliance with ethical standards

**Ethical statement** The study was reviewed and approved by the ethics committee of the First Affiliated Hospital of Xi'an Jiaotong University according to the Helsinki Declaration of 1975 (no. 20080301, 6 May 2008).

**Conflicts of interest** None.

#### References

1. Torre LA, Bray F, Siegel RL, Ferlay J, Lortet-Tieulent J, Jemal A. Global cancer statistics, 2012. *CA Cancer J Clin.* 2015;65:87–108.
2. Bruix J, Gores GJ, Mazzaferro V. Hepatocellular carcinoma: clinical frontiers and perspectives. *Gut.* 2014;63:844–55.
3. Zhong JH, Ke Y, Wang YY, Li LQ. Liver resection for patients with hepatocellular carcinoma and macrovascular invasion, multiple tumours, or portal hypertension. *Gut.* 2015;64:520–1.
4. Shimoda M, Tago K, Shiraki T, Mori S, Kato M, Aoki T, Kubota K. Risk factors for early recurrence of single lesion hepatocellular carcinoma after curative resection. *World J Surg* 2016.
5. Harada N, Shirabe K, Maeda T, Kayashima H, Takaki S, Maehara Y. Comparison of the outcomes of patients with hepatocellular



- carcinoma and portal hypertension after liver resection versus radiofrequency ablation. *World J Surg* 2016.
6. Zhang D, Lin J, Han J. Receptor-interacting protein (rip) kinase family. *Cell Mol Immunol*. 2010;7:243–9.
  7. Ofengeim D, Yuan J. Regulation of rip1 kinase signalling at the crossroads of inflammation and cell death. *Nat Rev Mol Cell Biol*. 2013;14:727–36.
  8. Festjens N, Vanden Berghe T, Cornelis S, Vandenabeele P. Rip1, a kinase on the crossroads of a cell's decision to live or die. *Cell Death Differ*. 2007;14:400–10.
  9. LaRocca TJ, Sosunov SA, Shakerley NL, Ten VS, Ratner AJ. Hyperglycemic conditions prime cells for rip1-dependent necroptosis. *J Biol Chem* 2016.
  10. Kelliher MA, Grimm S, Ishida Y, Kuo F, Stanger BZ, Leder P. The death domain kinase rip mediates the TNF-induced NF-kappaB signal. *Immunity*. 1998;8:297–303.
  11. Varfolomeev E, Vucic D. Unexpected roles of c-iaps in apoptotic and nfkappaB signaling pathways. *Cell Cycle*. 2008;7:1511–21.
  12. Darding M, Meier P. Iaps: guardians of ripk1. *Cell Death Differ*. 2012;19:58–66.
  13. Obitsu S, Sakata K, Teshima R, Kondo K. Eleostearic acid induces rip1-mediated atypical apoptosis in a kinase-independent manner via ERK phosphorylation, ros generation and mitochondrial dysfunction. *Cell Death Dis*. 2013;4:e674.
  14. Micheau O, Tschopp J. Induction of tnf receptor i-mediated apoptosis via two sequential signaling complexes. *Cell*. 2003;114:181–90.
  15. Ranjan K, Pathak C. Fadd regulates NF-kappaB activation and promotes ubiquitination of cflipl to induce apoptosis. *Sci Rep*. 2016;6:22787.
  16. Zheng X, Song T, Dou C, Jia Y, Liu Q. Ctbp2 is an independent prognostic marker that promotes gli1 induced epithelial-mesenchymal transition in hepatocellular carcinoma. *Oncotarget*. 2015;6:3752–69.
  17. Song T, Dou C, Jia Y, Tu K, Zheng X. Timp-1 activated carcinoma-associated fibroblasts inhibit tumor apoptosis by activating sdf1/cxcr4 signaling in hepatocellular carcinoma. *Oncotarget*. 2015;6:12061–79.
  18. Gai X, Lu Z, Tu K, Liang Z, Zheng X. Caveolin-1 is up-regulated by gli1 and contributes to gli1-driven EMT in hepatocellular carcinoma. *PLoS One*. 2014;9:e84551.
  19. Han W, Xie J, Fang Y, Wang Z, Pan H. Nec-1 enhances shikonin-induced apoptosis in leukemia cells by inhibition of rip-1 and erk1/2. *Int J Mol Sci*. 2012;13:7212–25.
  20. Gai X, Tu K, Lu Z, Zheng X. Mrc2 expression correlates with tgfbeta1 and survival in hepatocellular carcinoma. *Int J Mol Sci*. 2014;15:15011–25.
  21. Zheng X, Gai X, Ding F, Lu Z, Tu K, Yao Y, Liu Q. Histone acetyltransferase pcaf up-regulated cell apoptosis in hepatocellular carcinoma via acetylating histone h4 and inactivating AKT signaling. *Mol Cancer*. 2013;12:96.
  22. Wang L, Du F, Wang X. Tnf-alpha induces two distinct caspase-8 activation pathways. *Cell*. 2008;133:693–703.
  23. Zheng L, Bidere N, Staudt D, Cubre A, Orenstein J, Chan FK, Lenardo M. Competitive control of independent programs of tumor necrosis factor receptor-induced cell death by tradd and rip1. *Mol Cell Biol*. 2006;26:3505–13.
  24. Chen D, Yu J, Zhang L. Necroptosis: an alternative cell death program defending against cancer. *Biochim Biophys Acta*. 2016;1865:228–36.
  25. Qiu X, Klausen C, Cheng JC, Leung PC. Cd40 ligand induces rip1-dependent, necroptosis-like cell death in low-grade serous but not serous borderline ovarian tumor cells. *Cell Death Dis*. 2015;6:e1864.
  26. Zhang YF, He W, Zhang C, Liu XJ, Lu Y, Wang H, Zhang ZH, Chen X, DX X. Role of receptor interacting protein (rip) 1 on apoptosis-inducing factor-mediated necroptosis during acetaminophen-evoked acute liver failure in mice. *Toxicol Lett*. 2014;225:445–53.
  27. Huang C, Luo Y, Zhao J, Yang F, Zhao H, Fan W, Ge P. Shikonin kills glioma cells through necroptosis mediated by rip-1. *PLoS One*. 2013;8:e66326.
  28. Zhu G, Ye J, Huang Y, Zheng W, Hua J, Yang S, Zhuang J, Wang J. Receptor-interacting protein-1 promotes the growth and invasion in gastric cancer. *Int J Oncol*. 2016;48:2387–98.
  29. Zhu G, Chen X, Wang X, Li X, Du Q, Hong H, Tang N, She F, Chen Y. Expression of the rip-1 gene and its role in growth and invasion of human gallbladder carcinoma. *Cell Physiol Biochem*. 2014;34:1152–65.
  30. Liu XY, Lai F, Yan XG, Jiang CC, Guo ST, Wang CY, Croft A, Tseng HY, Wilmott JS, Scolyer RA, Jin L, Zhang XD. Rip1 kinase is an oncogenic driver in melanoma. *Cancer Res*. 2015;75:1736–48.